Self-Supported Polypyrrole/Polyvinylsulfate Films: Electrochemical Synthesis, Characterization, and Sensing Properties of Their Redox Reactions

Toribio F. Otero,*[a] Lluis X. Martinez-Soria,[a] Johanna Schumacher,[b] Laura Valero,[a, c] and Victor H. Pascual[a]

Thick films of polypyrrole/polyvinylsulfate (PPy/PVS) blends were electrogenerated on stainless-steel electrodes under potentiostatic conditions from aqueous solution. The best electropolymerization potential window was determined by cyclic voltammetry. After removing the film from the back metal, self-supported electrodes were obtained. Voltammetric, coulovoltammetric, and chronoamperometric responses from a LiClO4 aqueous solution indicated the formation of an energetically stable structure beyond a reduction threshold of the material. Its subsequent oxidation required higher anodic voltammetric overpotentials or longer chronoamperometric oxidation times. This structure was attributed to the formation of lamellar or vacuolar structures. X-ray photoelectron spectroscopy analysis of the films under different oxidations states revealed that the electrochemical reactions drive the reversible exchange of cations between the film and the electrolyte. The electrical energy and the charge consumed by the reversible reaction of the film under voltammetric conditions between the constant potential limits are a function of the potential scan rate, that is, they sense the working electrochemical conditions.

1. Introduction

In living beings, there are some organs that send information about the working conditions to the brain through continual feedback communication. This fact is what ultimately generates human proprioception.[1,2] Inside the intracellular matrix (ICM) of living cells, reactant macromolecules suffer conformational movements driven by reactions (molecular motors) that, at the same time, deliver electrical signals to the nervous system.[3,4] Living cells include a plethora of molecular motors.

The electrochemical devices developed in the last decades that are based on electroactive materials such as conducting polymers, graphenes, or carbon nanotubes, among others, work because of the electrochemical reactions that drive these basic materials.[5–9] These electrochemical reactions change the relative content(s) of the polymer/ions/solvent, which drives conformational movements (chemical molecular motors) of the constitutive chains and structures. They mimic those reactions occurring in the ICM of functional cells.[10,11] Biomimetic devices are being developed on the basis of these composition-dependent biomimetic properties; they include artificial muscles,[12–14] full polymeric batteries,[15–17] smart windows,[18–21] smart drug-delivery devices,[22–24] nervous interfaces,[25–27] smart membranes,[28,29] transducers,[30,31] biosensors,[32,33] and sensors.[34–36] These electrochemical biomimetic devices have a characteristic that has been attributed, so far, only to biological systems: they sense the working conditions during actuation.[37] This is a property of the reaction.

For an electrochemical device such as an actuator or a battery working under the flow of a constant current, the evolution of the device potential (potential difference between the working electrode, WE, and the counter electrode, CE) evolves through higher values if the device works at decreasing temperatures, in decreasing concentrations of the electrolyte, or under rising mechanical requirements, whereas the device moves between the same initial and final states (i.e. the same muscle positions or the same charged states of a battery).[38,39] One actuator and different sensors (thermal, chemical, electrochemical, or mechanical) work in concert in a physically uniform device driven by the same electrochemical reaction as that of the device's material (as it happens in haptic muscles). The electrochemical muscle is a Faradic motor, as the displacement rate is a linear function of the consumed charge.[6,11] The muscle potential is the sensing magnitude. This integration in

[a] Dr. T. F. Otero, L. X. Martinez-Soria, Dr. L. Valero, V. H. Pascual
Centre for Electrochemistry and Intelligent Materials (CEMI)
Universidad Politécnica de Cartagena (UPCT)
Aulario II, 30203 Cartagena (Spain)
E-mail: toribio.fotero@upct.es

[b] J. Schumacher
Arquimea Ingeniería S.L.U.
Calle Margarita Salas, 10 (Pol Ind Leganec)
28918 Leganés, Madrid (Spain)

[c] Dr. L. Valero
Engineering School, Universidad Autónoma del Estado de México
Toluca 50000 (Mexico)

The ORCID identification number(s) for the author(s) of this article can be found under http://dx.doi.org/10.1002/open.201600139.

one device of one motor and different sensors requires just two connecting wires for which all the actuating (current and charge) and the sensing (potential or consumed energy) magnitudes are simultaneously included. Sensing artificial muscles have led to the development and theoretical description of artificial proprioceptive devices.[24,40,41] The origin of the actuating and sensing abilities is the electrochemical reaction of the basic molecular motors: the polymeric chains or molecular and supramolecular carbonaceous structures. Electrochemical reactions from conducting polymers,[42–44] carbon nanotubes,[45] and graphenes[46] sense, by themselves, the working thermal, chemical, electrical, and mechanical conditions.

For the subsequent construction of sensing devices, thick films of electroactive materials are required such that reactions can sense the working conditions. This work is focused on the electrogeneration of thick films of the polymeric polypyrrole/ polyvinylsulfate (PPy/PVS) blend. The films are thick enough to be peeled off from the metal support without breaking. Those films are used as self-supported polymeric electrodes in aqueous electrolytes for the electrochemical characterization of the material. The ability of the reacting system to sense the electrochemical energy available for the material reaction under different scan rates, keeping the rest of the chemical and physical working conditions constant, will be presented here.

2. Results and Discussion

2.1. Electrosynthesis

Following the classical approach of electrochemical studies in aqueous solutions of any reactant, the potential window of the electrolyte (0.05 M NaPVS$_{(aq)}$) using a stainless steel (SS) WE was first obtained (green curve in Figure 1) by cyclic voltammetry at 40 mVs^{-1} between −1200 and 1000 mV. The voltammetric response shows that the system is stable between −1100 and 900 mV. At a more cathodic or anodic potential, water electrolysis occurs with hydrogen or oxygen evolution, respectively, over the SS electrode.

After the addition of the monomer to the electrolyte (0.1 M concentration of pyrrole), the consecutive voltammetric responses (red and pink curves in Figure 1) reveal that the monomeric oxidation polymerization begins beyond 650 mV on the
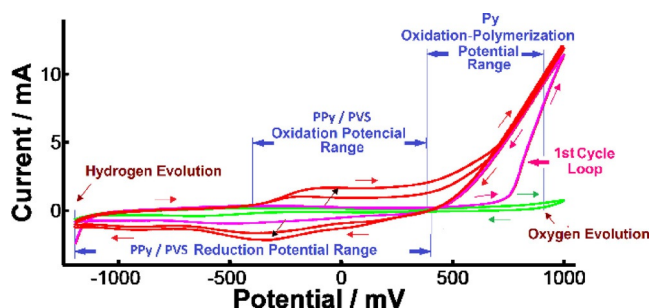
Figure 1. Voltammetric responses corresponding to the background electrolyte (0.05 M NaPVS aqueous solution): electrolyte potential window (——) and consecutive cycles in 0.1 M Py + electrolyte (—— and ——) at 40 mVs^{-1} between −1100 and 900 mV.

clean WE (pink curve) and above 400 mV if the metal is partially coated by the polymer (red curve) in the consecutive cycles. The first voltammetric response also indicates that the oxidation–polymerization begins by nucleation of the polymer on the metallic electrode, which gives a characteristic nucleation loop indicated in the first voltammogram. The generated polymer reduces between 400 and −1000 mV and reoxidizes beyond 400 mV. Thus, the monomeric oxidation–polymerization occurs in the potential range of 400 to 900 mV without any great interference of water electrolysis. Beyond 900 mV, polymer oxidation overlaps oxygen evolution from water.

Therefore, a constant potential of 800 mV was applied to a clean electrode in a fresh monomeric solution to synthesize the PPy/PVS polymeric blend until a uniform black polymeric film covered the metal and a polymerization charge of 0.5 C was consumed (Figure 2).
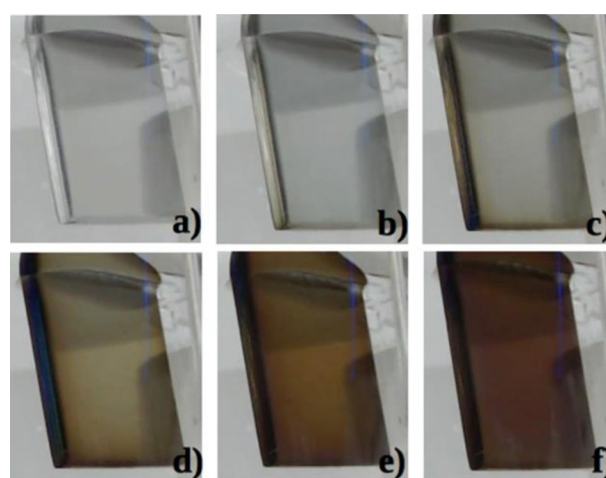
Figure 2. Stainless-steel working electrode submitted to 800 mV in 0.1 M Py and 0.05 M NaPVS aqueous solution for increasing times: a) 0 s, b) 5 s, c) 10 s, d) 20 s, e) 30 s, and f) 40 s showing how the electrogenerated brown film of PPy/PVS grows.

Afterwards, the potential was changed to 500 mV (inside the oxidation–polymerization potential range but far from the beginning of oxygen release) for 37 000 s, the time required to generate films thick enough to be peeled off from the metal. The final charge consumed during the electropolymerization process was 26.7 C. After generation, the film was rinsed several times with water and dried overnight in air. The mass of this oxidized film was 12.0 mg, which was obtained by weight difference between the weights of the coated and uncoated electrodes. By cutting the borders of the coated WE with a cutter, a film was peeled off from each side of the WE.

Finally, both films were cut into longitudinal strips. Each of those strips was prepared, as explained in the Experimental Section, to be used as a self-supported working electrode for its electrochemical characterization.

2.2. Electrochemical Characterization of the Polymer Blend

The self-supported electrodes were submitted to consecutive potential cycles and potential steps in 0.1 M LiClO$_4$ aqueous so-

lution. The film content was analyzed by X-ray photoelectron spectroscopy (XPS).

2.3. Voltammetric Responses from Different Cathodic Potential Limits

The self-supported electrodes were submitted to consecutive potential sweeps at 10 mVs^{-1} between a fixed anodic potential limit of 700 mV to a different cathodic potential limit, ranging from −600 to −1800 mV, every time. Steady-state voltammetric responses attained after two consecutive potential cycles show (Figure 3 a) a shift in the oxidation peak towards more anodic potentials for increasing cathodic potential limits. Any voltammetric response can be reproduced at any time by selecting the concomitant cathodic potential limit.
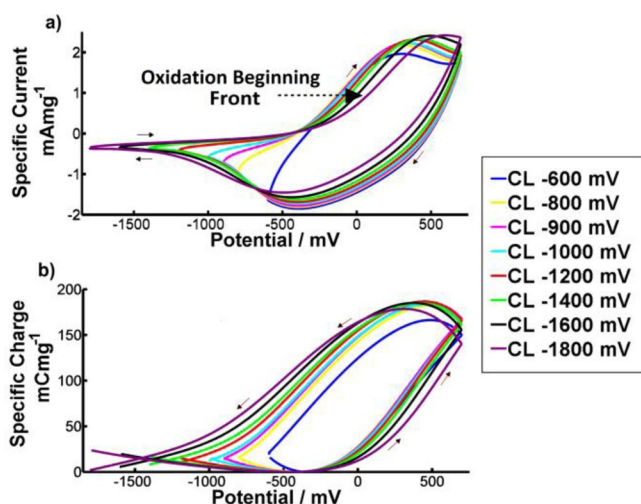
Figure 3. a) Stationary voltammetric responses from a self-supported PPy/PVS film immersed in a 0.1 M LiClO$_4$ aqueous solution and submitted to consecutive potential sweeps at 10 mVs^{-1} between the anodic potential of 700 mV and different cathodic potentials ranging from −600 to −1800 mV. b) Concomitant coulovoltammetric responses.

In the case of polymers exchanging cations during electrochemical reactions, the reduction at increasing cathodic over-potentials leads to the formation of more energetically stable structures such as lamellas, micelles, and vesicles.[47] Under constant temperature and at a constant electrolyte concentration, the only energetic source during the reaction is the applied potential. The more energetically stable structures attained by reduction at increasing cathodic potentials can only be reoxidized on the subsequent anodic potential sweeps at increasing electrochemical energies: the subsequent oxidation peak shifts towards more anodic potentials.[48–50] The reduction peaks always maintain the same positions, regardless of the cathodic potential limit, because complete oxidation of the polymeric film during the oxidation peak erases any energetic memory reached by reduction until different cathodic potential limits. Thus, the cathodic potential sweep always starts from the same oxidized energetic structure.

By integration of the voltammetric responses (current–potential, I–E), the coulovoltammetric (charge-potential, Q–E) re-

sponses are attained (Figure 3 b). The slopes (Q/E) of the coulovoltammograms indicate the electrochemical reaction rate.[51] Positive charge increases between two points mean oxidation charges and negative charge increments account for reduction charges.

In Figure 3 b it can be appreciated that the reversible charge (difference between the coulovoltammetric maximum and minimum, Q$_{rev}$) first increases upon increasing the cathodic potential limit and then decreases for the highest-studied cathodic potential limits. This decrease is due to partial reoxidation of the reduced material at the anodic limit of 700 mV, which is caused by anodic shift of the oxidation peak to higher anodic potentials. Consequently, only a fraction of the energetically stable structures reached by reduction is reoxidized during the subsequent anodic potential sweep.

The change in the slope on the reduction branch of the coulovoltammetric responses at high cathodic potentials is attributed to the formation of lamellas or vesicles after a reduction threshold.[47] The formation of these energetically stable structures goes on by electrochemical reduction (decreasing charges on Figure 3 b) at the beginning of the subsequent oxidation branch until the Q–E minimum. Similar effects for increasing cathodic limits have been observed in polymers exchanging anions.[49]

2.4. Reaction-Driven Ionic Exchange

The PPy/PVS blend is expected to exchange cations during reactions in aqueous solutions, but the potential shifts observed in Figure 3 a can also be found in conducting polymers exchanging anions with the electrolyte during electrochemical reactions. To determine the ionic exchange (anions or cations) driven by the electrochemical reaction, three films of PPy/PVS (directly after synthesis, after voltammetric oxidation, and after voltammetric reduction) were analyzed by XPS. Figure 4 presents the attained results (overlapped).

The oxidized and reduced sates were attained after potential cycling between 500 and −800 mV at 10 mVs^{-1} in 0.1 M NaClO$_4$ aqueous solutions (the available equipment did not detect Li$^+$). After submission to consecutive potential sweeps, the potential was stopped at −800 mV to obtain a reduced state of the film and at 500 mV to obtain an oxidized state of the second film. After rinsing and drying the films were analyzed.
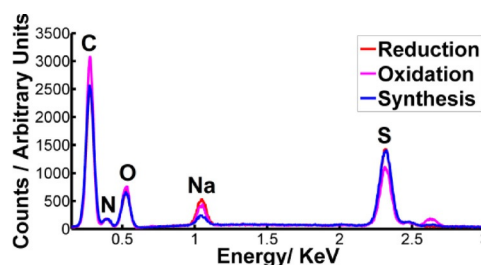
Figure 4. XPS analysis of three PPy/PVS films: after film synthesis, after potential cycling stopping the potential sweep at −800 mV (reduced film), and after stopping the potential cycling at 500 mV (oxidized state). The background was a 0.1 M NaClO$_4$ aqueous solution.

A higher cation (Na$^+$) content was observed in the reduced polymer. None of the three studied samples contained Cl from the ClO$_4^-$ anion. These facts indicate that under the studied conditions the electrochemical oxidation/reduction reactions of PPy/PVS films drive the exchange of cations with the electrolyte by following the oxidation/reduction reactions [Eq. (1)]:

$$\left[(PPy)_{(s)}(PVS^-Na^+)_n(H_2O)_m\right] \\ \leftrightarrow (PPy^{n+})(PVS^-)_n + n\,Na^+ + m\,(H_2O) + n\,e^- \qquad (1)$$
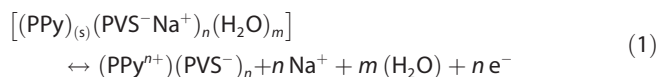
in which PPy represents the chain's active centers that will store a positive charge after oxidation, subindex s implies solid, PVS$^-$ represents the anion trapped in the film during its electrogeneration, Na$^+$ is the exchanged cation driven by the oxidation/reduction reactions to keep the charge balance in the film, and water molecules are exchanged for osmotic balance.
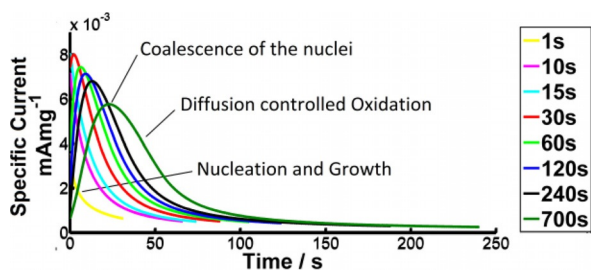
The exchanged solvent can play an important role in the electrochemical activity of blends of conducting polymers with polyelectrolytes. Using acetonitrile, instead of water, the reaction drives the exchange of anions.[52,53]

2.5. Influence of the Initial Reduction Time on the Chronoamperometric Responses

Given that the increasing cathodic potential limit has a profound influence in the subsequent oxidation reaction, a different approach was then taken by using chronoamperometric responses to study the influence of the deep reduction of the blend.

The self-supported electrode, after oxidation at 500 mV, was reduced at −800 mV for different times for each experiment. Then the potential was stepped to 500 mV. This potential was kept for enough time to obtain a "full" oxidation state of the film (the current dropped close to zero) at that potential. Figure 5 shows the anodic chronoamperometric responses after different reduction times.

The chronoamperometric responses show a minimum and a maximum, which are characteristic of the nucleation and coalescence processes, respectively.[54] For conducting polymer blends doped with large polymeric anions such as polyvinylsulfonate (PVS$^-$), these large anions remain trapped and entangled within the polypyrrole chains during the oxidation/reduction processes.[9]

The film swells during reduction: electrons are injected into the CP, which eliminates positive charges on the PPy chains, and cations are forced to penetrate from the solution to balance the PVS$^-$ charges with parallel entrance of solvent for osmotic balance. The film shrinks by oxidation. At high reduction potentials, it has been proposed[55–57] that the contents of water, cations, and PVS are high enough to form nanolamellar or nanovacuolar structures surrounded by deeply reduced and compacted PPy.

During the subsequent oxidation process, the PVS$^-$ chain fractions forming the lamellar structure must migrate back into the packed PPy, which requires a nucleation process. The nucleation maximum shifts towards lower currents and higher oxidation times after increasing the reduction times, which results in rising reduced and conformational compacted structures.

After short reduction times (below 30 s), the chronoamperograms exhibit Cottrell evolution of the current decay.[58] After reduction times higher than 30 s, the responses present a chronoamperometric maximum, which suffers displacement towards lower currents and higher oxidation times with increasing initial reduction times. The chronoamperometric minimum and maximum are characteristic of the formation and coalescence of nuclei of the oxidized polymer, respectively, through the reduced structure.[41,59,60] Deeper reduced and conformational compacted initial energetic structures require longer nucleation and coalescence times by oxidation at a constant potential (constant electrochemical energy). After full oxidation of the PPy/PVS material, any maximum from Figure 5 can be repeated as many times as wished by using the concomitant reduction time.
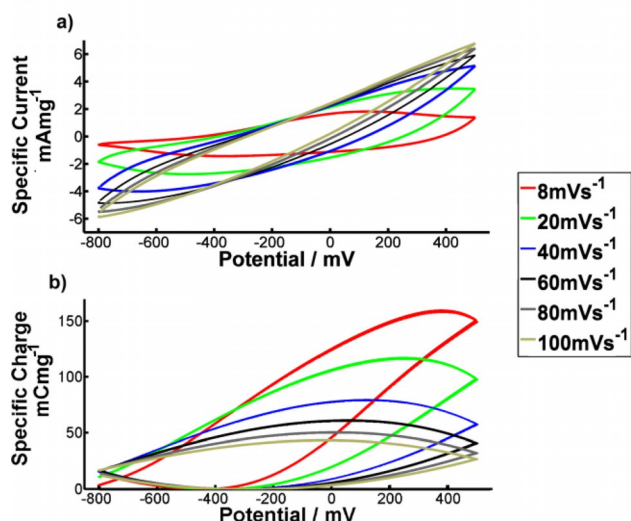
The nucleation process is reproducible, and its visual observation is possible by using thin electrochromic films of conducting polymers on mirror-polished metal electrodes.[54,61]

2.6. Influence of the Scan Rate

The stationary voltammetric responses corresponding to different scan rates between 8 and 100 mVs^{-1} are displayed by Figure 6a.

Below 20 mVs^{-1}, the oxidation and reduction maxima are clearly observed. Above those values the voltammetric maxima disappear. The oxidation and reduction maxima show strong anodic and cathodic potential shifts for increasing scan rates, respectively (Figure 6a). As a result, the potential difference between these two peaks (electrochemical hysteresis) increases with the potential sweep rate. This effect indicates that the resistance gradient between oxidative shrinking of the film, which drives the cation's ejection [see Eq. (1), forwards reaction] from inside the film towards the solution, and its reductive swelling, which drives the entrance of the cations from the solution [See Eq. (1), backwards reaction], increases with increasing scan rates.

These voltammetric responses can be presented as coulovoltammetric responses (Figure 6b). The potentiostat/galvanostat

Figure 5. Chronoamperometric responses from a free-standing PPy/PVS film immersed in 0.1 M LiClO$_4$ aqueous solution after reduction at −800 mV for different times and then stepping the potential to 500 mV for the time required to "complete" film oxidation (the anodic current drops close to zero).

Figure 6. a) Stationary voltammetric responses attained from free-standing PPy-PVS films at different scan rates ranging from 8 to 100 mVs⁻¹ between −800 and 500 mV in a 0.1 M LiClO₄ aqueous solution. b) Concomitant coulo-voltammograms.

used here gives both responses. Positive charge increases between two points mean oxidation charges and negative charge increments mean reduction charges. Most of the Q–E responses show a closed loop. In the loop, the positive charges equal the negative charges, which means that the reactions are reversible. The charge difference between the loop maximum and the minimum is the charge involved for reversible oxidation/reduction of the film during each potential sweep.

The reversible charge decreases upon increasing the scan rate for the whole potential range studied (Figure 7a). Working at constant temperature (constant thermal energy) and at
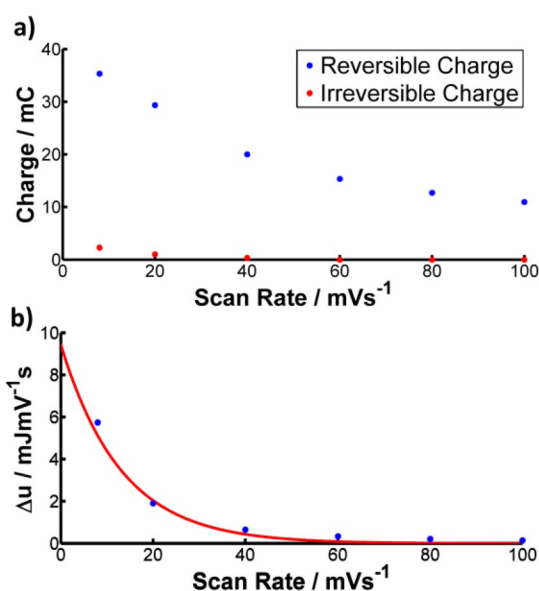
Figure 7. a) Evolution of the two components of the consumed charge, reversible and irreversible, from the coulovoltammetric responses depicted by panel b as a function of scan rate. b) Evolution of the effective consumed electrical energy with the scan rate.

a constant electrolyte concentration (constant chemical energy), upon increasing the scan rate, cycling the potential between the same potential limits results in less electrochemical energy available per potential cycle. As a consequence, extension of the reaction (the charge consumed by the reversible and irreversible reactions) decreases: less charge is consumed by Equation (1) and less hydrogen evolves at higher potential scan rates. The coulovoltammetric open part on the left side observed at the lower scan rate represents the irreversible charge. This is the charge consumed by irreversible reactions (hydrogen evolution[47]) occurring in parallel to film reduction at high cathodic potentials. The irreversible charge increases for decreasing scan rates (Figure 7a) in the potential range studied.

According to the electrochemically stimulated conformational relaxation (ESCR) model, for those scan rates the reaction should occur under diffusion kinetic control of the counter ions (cations) through the film.[62, 63]

If all the other parameters (temperature, electrolyte concentration, and so on) remain constant, by sweeping the potential between the same potential limits defining the same potential range (ΔE), the effective electrochemical energy (Δu) applied to the reacting polymeric film for different potential scan rates (v) is [Eq. (2)]:

$$\Delta u = \frac{\Delta V \ [\text{J}]}{v \ [\text{V s}^{-1}]} = \Delta Q_{rev} \ [\text{C}] \frac{\Delta Q_{rev} \cdot \Delta E}{v} \ [\text{C s}] \qquad (2)$$

in which Q, the consumed charge, according to the ESCR model, is described by an exponential function of v.[50, 64]

Upon increasing the scan rate, the reversible charge (Q_{rev}) involved in Equation (1) decreases and the effective potential gradient ($\Delta E/v$) also decreases: the available and consumed electrochemical energy (Δu) decreases faster than the two other parameters. Figure 7b shows the empirical evolution of the effective electrical energy consumed by the reversible oxidation/reduction of the PPy/PVS film as a function of the applied scan rate. The experimental results fit Equation (3):

$$\Delta u = a e^{bv} \qquad (3)$$

in which $a = 11.14$ mJ mV⁻ s, $b = -0.084$ mC⁻¹, and the correlation coefficient is $r^2 = 0.99$.

According to the ESCR model, the voltammetric responses are described by two exponential functions related to the conformational compaction/relaxation of the polymeric chains and to the diffusion of ions during the reaction-driven swelling–shrinking of the film. At high scan rates, the film reactions do not have (inside the studied potential range) enough time to attain film oxidation/compaction and subsequent reduction/relaxation. Only at low scan rates do the film reactions have enough time to attain these processes. Under the studied conditions, the reaction occurs under diffusion kinetic control, and the electrical energy consumed by the reaction follows the exponential function [Eq. (3)] of the sweep rate.

The final result is that both the electrical energy [Eq. (3)] consumed by the reversible reaction from Equation (1) and the

charge required to oxidize/reduce the PPy/PVS film in a reversible way (Figure 8a) are a function of the experimental scan rate, that is, the working electrochemical energetic conditions. Thus, by cycling between the constant potential limits, the electrical energy and the charge consumed by reversible oxidation/reduction of the material both sense the working electrochemical conditions: they sense the applied sweep rate.
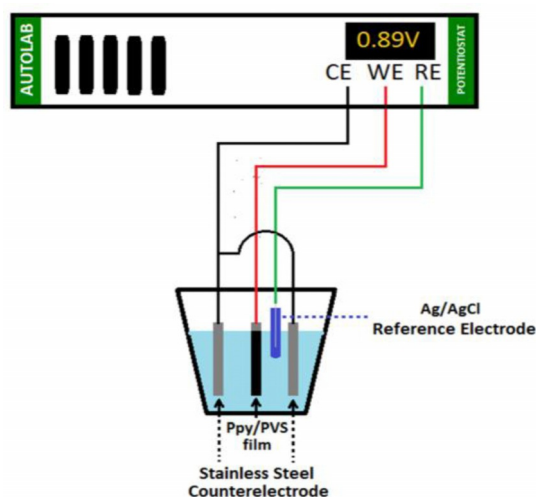
Figure 8. Schematic representation of the electrochemical cell used for polymeric synthesis.

3. Conclusions

Thick polymeric blend (polypyrrole/polyvinylsulfate, PPy/PVS) films were electrogenerated under constant potential by polarization of a stainless-steel electrode at 800 mV until metal coating and then at 500 mV for the time required to consume 27.2 C. The two thick films (one by steel side) were peeled off from the electrode and cut into longitudinal strips to obtain self-supported electrodes. The voltammetric responses showed structural changes upon increasing the cathodic potential limits, which resulted in a reduced material with increasingly energetically stable structures. As a consequence, the beginning of their oxidation on subsequent anodic branches required increased anodic overpotentials. Oxidation by potential steps gave oxidation–nucleation maxima at lower currents and increased times after reduction for higher reduction times. XPS analysis of the films under different oxidation states proved that the exchange of cations with the electrolyte was driven by oxidation/reduction of the film, as described in Equation (1). As it happens for other polymeric blends of conducting polymers with polyelectrolytes or with large organic anions, the structural changes observed at high cathodic potentials were attributed to the formation of lamellar or vacuolar structures in the film beyond a reduction threshold. Voltammetric experiments performed at increasing sweep rates showed that both the effective electrical energy and the charge consumed by the reversible reaction presented in Equation (1) were a function of the sweep rate [Eq. (2)]. Consequently, both the charge and the electrical energy consumed by reactions involving conformational and structural transformations of the polymeric reactants act as sensors for the working electrochemical energetic conditions. Equation (3) is the sensing equation. Thus, any electrochemical device (e.g. artificial muscle, battery, electrochromic window, smart membrane, and nervous interface) constituted by PPy/PVS and driven by this reaction will simultaneously be a sensor of the working electrochemical conditions.

Experimental Section

Chemicals

The monomer pyrrole (Sigma–Aldrich, 98%) was purified by distillation under vacuum at 7 mbar and 42°C and was stored under dark conditions at −10°C before use. Poly(vinylsulfonic acid, sodium salt) solution (NaPVS) (Sigma–Aldrich, 25 wt% in H_2O), lithium perchlorate ($LiClO_4$) (Sigma–Aldrich, 95%), and sodium perchlorate ($NaClO_4$) (Sigma–Aldrich, 98%) were used as supplied. Ultrapure water from Millipore Milli-Q equipment was employed to prepare the solutions.

Electrochemical measurements were performed by using a potentiostat-galvanostat AUTOLAB PGSTAT302 controlled by NOVA 1.11 software and a three-electrode electrochemical cell configuration. The reference electrode (RE) was Ag|AgCl (KCl 3 M) from Metrohm. The potentials in this paper are referred to this electrode. For electropolymerization, the cell contained two counter electrodes (CEs) and a working electrode (WE) of stainless steel (SS) AISI 316 (see Figure 8) with an immersed surface area of 3.64 cm² each side. The two CEs were placed symmetrically at both sides of the WE to ensure uniform deposition of the polymer on each side of the WE plate. Before each electropolymerization, the cell was closed and purged with nitrogen for 20 min.

For electrochemical characterization, one CE of SS AISI 316 and a self-supported PPy/PVS film as the WE were employed in 0.1 M $LiClO_4$ aqueous solutions. A Sartorius Extended ED224s balance was used to weigh the films, and an electronic microscope Hitachi S.3500N was used for X-ray photoelectron spectroscopy (XPS) analysis.

Preparation of Self-Support Electrodes

After electropolymerization, the surface areas of the generated films were measured. With the polymer mass, the deposited mass per unit of area was determined. Then, the polymer films were peeled off from the metal electrode and cut into longitudinal strips. Self-supported electrodes were prepared by painting a transversal line, with a width of 1 mm, around the polymer strip and close to the film top. The paint closed the polymer pores, which therefore avoided movement of the solution by capillarity towards the metallic electric contact at the top and, at the same time, allowed good electronic conductivity through it.[65] The film was immersed into the electrolyte by keeping the transversal paint strip above the solution. This mark was also used to know, at all times, the surface area (and therefore the mass) of the polymer immersed and involved in the electrochemical reactions. Currents and charges measured during the electrochemical characterizations were transformed into specific currents, I_{spe} [mA mg^{-1}], and specific charges, Q_{spe} [mC mg^{-1}].

Electrochemical Characterization Methodology

The film used to obtain the experimental results must keep the same electroactivity during the full experimental series. Film electroactivity was controlled by cyclic voltammetry: before and after each experiment the film was cycled at a scan rate of 10 mVs^{-1} between -800 and 500 mV in the background electrolyte. Deviation of the charge involved in the film redox process or reversible charge (Q_{rev}) was always lower than 7%. Consequently, the same electroactive material was used during the experimental series. If a voltammetric control gave a higher variation in the involved charge, this film was discarded and a new PPy/PVS film was prepared to continue with the experimental series.

Steady-state electrochemical responses (voltamperometric and coulovoltammetric) from the polymeric electrode, after it was submitted to consecutive potential cycles, were considered as representative of the voltammetric control. In this way, any material memory[10,48,66] from the electrogeneration process or from previous experiences were erased.

The influence of any treatment on the voltammetric or chronoamperometric responses from the material was studied from the first of those responses.

Acknowledgements

Conflict of Interest

The authors declare no conflict of interest.

[1] J. A. Ashton-Miller, E. M. Wojtys, L. J. Huston, D. Fry-Welch, *Knee Surg. Sports Traumatol. Arthrosc.* **2001**, *9*, 128 – 136.

[2] J. R. Lackner, P. DiZio, "Vestibular, Proprioceptive, and Haptic Contributions to Spatial Orientation" in *Annual Review of Psychology, Vol. 56*, Annual Reviews, Palo Alto, **2005**, pp. 115 – 147.

[3] J.-G. Barbara, F. Clarac, *Brain Res.* **2011**, *1409*, 3 – 22.

[4] G. G. Matthews, *Cellular Physiology of Nerve and Muscle*, Wiley-Blackwell, Hoboken, NJ, **2009**.

[5] T. F. Otero, *Conducting Polymers: Bioinspired Intelligent Materials and Devices*. Royal Society of Chemistry, London, **2015**.

[6] T. F. Otero, *Polym. Rev.* **2013**, *53*, 311 – 351.

[7] Y. Bar-Cohen, *Electroactive Polymer (EAP) Actuators as Artificial Muscles: Reality, Potential, and Challenges*, SPIE Press, Bellingham, WA, **2001**.

[8] G. G. Wallace, G. M. Spinks, L. A. P. Kane-Maguire, *Conductive Electroactive Polymers: Intelligent Polymer Systems*, 3rd ed., CRC Press, London, **2008**.

[9] T. F. Otero, J. G. Martinez, *J. Mater. Chem. B* **2016**, *4*, 2069 – 2085.

[10] T. F. Otero, J. G. Martinez, *J. Mater. Chem. B* **2013**, *1*, 26 – 38.

[11] T. F. Otero, J. G. Martinez, J. Arias-Pardilla, *Electrochim. Acta* **2012**, *84*, 112 – 128.

[12] T. Otero, E. Angulo, J. Rodriguez, C. Santamaria, *J. Electroanal. Chem.* **1992**, *341*, 369 – 375.

[13] Q. Pei, O. Inganas, *Adv. Mater.* **1992**, *4*, 277 – 278.

[14] T. Mirfakhrai, J. D. W. Madden, R. H. Baughman, *Mater. Today* **2007**, *10*, 30 – 38.

[15] J. A. Irvin, D. J Irvin, J. D Stenger-Smith, *Electroactive Polymers for Batteries and Supercapacitors in Conjugated Polymers, Vol. 2*, CRC Press, Boca Raton, FL, **2006**, pp. 1 – 29.

[16] P. Novák, K. Muller, K. S. V. Santhanam, O. Haas, *Chem. Rev.* **1997**, *97*, 207 – 281.

[17] R. Gracia, D. Mecerreyes, *Polym. Chem.* **2013**, *4*, 2206 – 2214.

[18] V. K. Thakur, G. Ding, J. Ma, P. S. Lee, X. Lu, *Adv. Mater.* **2012**, *24*, 4071 – 4096.

[19] D. R. Rosseinsky, R. J. Mortimer, *Adv. Mater.* **2001**, *13*, 783.

[20] C. M. Amb, A. L. Dyer, J. R. Reynolds, *Chem. Mater.* **2011**, *23*, 397 – 415.

[21] P. M. Beaujuge, J. R. Reynolds, *Chem. Rev.* **2010**, *110*, 268 – 320.

[22] M. R. Abidian, D. H. Kim, D. C. Martin, *Adv. Mater.* **2006**, *18*, 405 – 409.

[23] C. Alvarez-Lorenzo, A. Concheiro, *Curr. Opin. Biotechnol.* **2013**, *24*, 1167 – 1173.

[24] J. Kost, R. Langer, *Adv. Drug Delivery Rev.* **2001**, *46*, 125 – 148.

[25] R. A. Green, N. H. Lovell, G. G. Wallace, L. A. Poole-Warren, *Biomaterials* **2008**, *29*, 3393 – 3399.

[26] R. Green, M. R. Abidian, *Adv. Mater.* **2015**, *27*, 7620 – 7637.

[27] M. Asplund, T. Nyberg, O. Inganas, *Polym. Chem.* **2010**, *1*, 1374 – 1391.

[28] M. J. Ariza, T. F. Otero, *Colloids Surf. Physicochem. Eng. Asp.* **2005**, *270*, 226 – 231.

[29] J. Pellegrino, "The Use of Conducting Polymers in Membrane-Based Separations: A Review and Recent Developments" in *Annals of the New York Academy of Sciences, Vol. 984: Advanced Membrane Technology* (Eds.: N. N. Li, E. Drioli, W. S. W. Ho, G. G. Lipscomb), New York Academy Sciences, New York, **2003**, pp. 289 – 305.

[30] R. Tiwari, E. Garcia, *Smart Mater. Struct.* **2011**, *20*, 083001.

[31] D. Pugal, K. Jung, A. Aabloo, K. J. Kim, *Polym. Int.* **2010**, *59*, 279 – 289.

[32] C. Dhand, M. Das, M. Datta, B. D. Malhotra, *Biosens. Bioelectron.* **2011**, *26*, 2811 – 2821.

[33] M. Gerard, A. Chaubey, B. D. Malhotra, *Biosens. Bioelectron.* **2002**, *17*, 345 – 359.

[34] L. Valero Conzuelo, J. Arias-Pardilla, J. V. Cauich-Rodriguez, M. Afra Smit, T. Fernandez Otero, *Sensors* **2010**, *10*, 2638 – 2674.

[35] N. Gupta, S. Sharma, I. A. Mir, D. Kumar, *J. Sci. Ind. Res.* **2006**, *65*, 549 – 557.

[36] T. Wang, M. Farajollahi, Y. Sik Choi, I.-T. Lin, J. E. Marshall, N. M. Thompson, S. Kar-Narayan, J. D. W. Madden, S. K. Smoukov, *Interface Focus* **2016**, *6*, 20160026.

[37] T. F. Otero, J. G. Martinez, *Prog. Polym. Sci.* **2015**, *44*, 62 – 78.

[38] J. G. Martinez, T. F. Otero, *J. Phys. Chem. B* **2012**, *116*, 9223 – 9230.

[39] T. F. Otero, J. J. Sanchez, J. G. Martinez, *J. Phys. Chem. B* **2012**, *116*, 5279 – 5290.

[40] G. G. Matthews, *Cellular Physiology of Nerve and Muscle*, 4th ed., Wiley-Blackwell, Hoboken, NJ, **2016**.

[41] Q. Pei, O. Inganas, *J. Phys. Chem.* **1992**, *96*, 10507 – 10514.

[42] S. Cosnier, M. Holzinger, *Chem. Soc. Rev.* **2011**, *40*, 2146 – 2156.

[43] Y. A. Ismail, J. G. Martinez, A. S. Al Harrasi, S. J. Kim, T. F. Otero, "Polypyrrole/Chitosan Hydrogel Hybrid Microfiber as Sensing Artificial Muscle" in *Electroactive Polymer Actuators and Devices (eapad) 2011, Vol. 7976* (Eds.: Y. BarCohen, F. Carpi), Spie-Int. Soc Optical Engineering, Bellingham, WA, **2011**, p. 79761L.

[44] Y. A. Ismail, J. G. Martinez, A. S. Al Harrasi, S. J. Kim, T. F. Otero, *Sens. Actuators B* **2011**, *160*, 1180 – 1190.

[45] J. G. Martínez, T. Sugino, K. Asaka, T. F. Otero, *ChemPhysChem* **2012**, *13*, 2108 – 2114.

[46] J. G. Martínez, T. F. Otero, C. Bosch-Navarro, E. Coronado, C. Marti-Gastaldo, H. Prima-Garcia, *Electrochim. Acta* **2012**, *81*, 49 – 57.

[47] T. F. Otero, J. G. Martinez, M. Fuchiwaki, L. Valero, *Adv. Funct. Mater.* **2014**, *24*, 1265 – 1274.

[48] M. Fuchiwaki, T. F. Otero, *J. Mater. Chem. B* **2014**, *2*, 1954 – 1965.

[49] T. F. Otero, M. Alfaro, V. Martinez, M. A. Perez, J. G. Martinez, *Adv. Funct. Mater.* **2013**, *23*, 3929 – 3940.

[50] T. F. Otero, H. Grande, J. Rodriguez, *J. Phys. Chem. B* **1997**, *101*, 8525 – 8533.

[51] T. F. Otero, *Electrochim. Acta* **2016**, *212*, 440 – 457.

[52] A. J. Fernández Romero, J. J. López Cascales, T. Fernández Otero, *J. Phys. Chem. B* **2005**, *109*, 907 – 914.

[53] R. Kiefer, J. G. Martinez, A. Keskula, G. Anbarjafari, A. Aabloo, T. F. Otero, *Sens. Actuators B* **2016**, *233*, 328 – 336.

[54] T. F. Otero, I. Boyano, *ChemPhysChem* **2003**, *4*, 868 – 872.

[55] B. J. West, T. F. Otero, B. Shapiro, E. Smela, *J. Phys. Chem. B* **2009**, *113*, 1277 – 1293.

[56] W. Wernet, M. Monkenbusch, G. Wegner, *Makromol. Chem. Rapid Commun.* **1984**, *5*, 157 – 164.

[57] K. Naoi, Y. Oura, M. Maeda, S. Nakamura, *J. Electrochem. Soc.* **1995**, *142*, 417 – 422.

[58] I. J. Suárez, T. F. Otero, M. Márquez, *J. Phys. Chem. B* **2005**, *109*, 1723 – 1729.

[59] J. G. Martinez, T. F. Otero, *RSC Adv.* **2014**, *4*, 29139 – 29145.

[60] T. F. Otero, I. Boyano, *J. Phys. Chem. B* **2003**, *107*, 6730 – 6738.

[61] T. F. Otero, H. J. Grande, J. Rodriguez, *J. Phys. Chem. B* **1997**, *101*, 3688 – 3697.

[62] T. F. Otero, M. J. Ariza, *J. Phys. Chem. B* **2003**, *107*, 13954 – 13961.

[63] H. Grande, T. F. Otero, *Electrochim. Acta* **1999**, *44*, 1893 – 1900.

[64] H. Grande, T. F. Otero, *J. Phys. Chem. B* **1998**, *102*, 7535 – 7540.

[65] M. Fuchiwaki, J. G. Martinez, T. F. Otero, *Adv. Funct. Mater.* **2015**, *25*, 1535 – 1541.

[66] C. Barbero, R. Kotz, M. Kalaji, L. Nyholm, L. Peter, *Synth. Met.* **1993**, *55*, 1545 – 1551.